6986 J. Med. Chem. 2010, 53, 6986–6995
DOI: 10.1021/jm1006269

Journal of Medicinal Chemistry Article

Rigid Analogues of the α2-Adrenergic Blocker Atipamezole: Small Changes, Big Consequences

Bernard Vacher,*,† Philippe Funes,† Philippe Chopin,‡ Didier Cussac,§ Peter Heusler,§ Amelie Tourette,§ and Marc Marien‡

†Medicinal Chemistry 1 Division, ‡Neurobiology 1 Division, and §Cellular and Molecular Biology Department, Pierre Fabre Research Center, 17 Avenue Jean Moulin, 81106 Castres Cedex, France

Received May 24, 2010

We report the discovery of a new family of α_2 adrenergic receptor antagonists derived from atipamezole. Affinities of the compounds at human α_2 and α_{1b} receptors as well as their functional activities at $h\alpha_{2A}$ receptors were determined in competition binding and G-protein activation assays, respectively. Central α_2 antagonist activities were confirmed in mice after oral administration. Further studies on a selected example: (+)-4-(1a,6-dihydro-1*H*-cyclopropa[a]inden-6a-yl)-1*H*-imidazole, (+)-**1** (F 14805), were undertaken to probe the potential of the series. On the one hand, (+)-**1** increased the release of noradrenaline in mouse frontal cortex following acute systemic administration, the magnitude of this effect being much larger than that obtained with reference agents. On the other, (+)-**1** produced minimal cardiovascular effects in intact, anesthetized rat, a surprising outcome that might be explained by its differential action at peripheral and central α_2 receptors. A strategy for improving the therapeutic window of α_2 antagonists is put forward.

Introduction

α Adrenergic receptors are widely distributed in the periphery and central nervous systems (CNS[a]). They are divided into two subclasses designated as α_1 and α_2.[1] α_1 Receptors are primarily located postjunctionally, whereas α_2 receptors are located at both pre- and postsynaptic levels.[2] More than half of the total number of noradrenergic neurons in the CNS is contained in the locus-coeruleus (LC), which provides the bulk of noradrenaline (NA) found in the brain and spinal cord. By blocking inhibitory presynaptic α_2 receptors in LC, antagonists disinhibit LC neurons, leading to increases in firing rate, NA synthesis, and release.[3] α_2 Antagonists also facilitate the activity of neuronal and glial targets downstream from the LC.[4] Those combined actions appear to afford resistance and promote recovery in response to experimental neural insult or injury. As such, α_2 antagonists have been proposed as a therapeutic strategy not only to relieve symptoms but also to retard the evolution of neurodegenerative disorders.[4] Some clinical evidence are consistent with this.[5] For instance, idazoxan[6] improved motor performance in Parkinson's disease (PD)[7] and in progressive supranuclear palsy.[8] It also reversed attention deficits in patients with dementia[9] and enhanced cerebrocortical glucose metabolism in man.[10,11] Fipamezole,[12] a fluoro-analogue of atipamezole, has shown positive effects in a phase IIb trial for reducing L-dopa induced dyskinesias in PD.[13,14]

The human α_2 receptor population is itself heterogeneous, and several subtypes, termed α_{2A}, α_{2B}, and α_{2C}, have been identified to date.[15] The α_{2A} subtype is the prominent α_2 receptor in the brain and dorsal horn, and it mediates most of the central effects of α_2 agonists. The α_{2C} receptor is present in the CNS albeit as a minor population, and on peripheral adrenergic terminals. The α_{2B} subtype is essentially expressed at a postsynaptic level on vascular tissue. Historically, the development of α_2 antagonists has been plagued by their cardiovascular activity. The three α_2 subtypes are implicated in hemodynamic regulation: α_{2B} and α_{2A} receptors in arterial contraction, and α_{2C} in venous vasoconstriction.[16] In this work, α_2 subtype selectivity was not used as a selection criterion.

The structures of the molecules that block α_2 receptors are highly diverse, ranging from small, poorly functionalized, achiral ones, e.g., atipamezole[17a] to large, complex alkaloids such as yohimbine[18] (Figure 1). There is thus no shortage of leads.[19] Herein we provide an account of our effort to discover rigid analogues of atipamezole, a selective antagonist of both central and peripheral α_2 receptors[17b] used in veterinary care. At the outset, a cyclopropyl[*a*]Indane template was deemed ideal for studying the relationship between conformation and activity in atipamezole-like molecules on the premise that: (1) structural changes relative to atipamezole could be kept minimal, and (2) the 3D-shape could be perfectly defined except for the orientation of the imidazole ring (Figure 2).[20] In this respect, appending a substituent at positions 1, 1a, or 6 on the bicyclo[3.1.0]heptane backbone was expected to narrow down the number of conformers, a feature that we intended to exploit to gain new insights into the geometry of the antagonist bound state(s) (Table 1).[21]

In the first part of this work, we examined the influence of substituents placed at C1, C1a, or C6 on in vitro and in vivo parameters using atipamezole and fipamezole as benchmarks. We next focused on a specific member of the series, (+)-**1**, and

*To whom correspondence should be addressed. Phone: (+33) 56371 4222. Fax: (+33) 56371 4299. E-mail: bernard.vacher@pierre-fabre.com.

[a] Abbreviations: CNS, central nervous system; LC, locus-coeruleus; NA, noradrenaline; PD, Parkinson's disease; NMN, normetanephrine; DAP, diastolic arterial blood pressure; ip, intraperitoneal route of administration; po, oral route of administration; SNRI, selective NA reuptake inhibitor.

 Published on Web 09/01/2010

compared its NA-releasing properties to that of atipamezole, fipamezole, and desipramine. Finally, we discussed the cardiovascular profile of (+)-**1** in rat models and the important mechanistic aspects that emerged from it.

Chemistry

We have previously published the preparation of the key intermediate **16** along with that of derivatives **1**, **10**−**15**.[22] The synthesis of compounds **2**−**6** is depicted in Scheme 1. Reduction of the ketone in **16** with potassium borohydride occurred diastereoselectively, the hydride entering from the same side as the ester group to afford the (6*S**,6a*S**)-alcohol **17**.[23] *O*-Alkylation of the hydroxyl function with the appropriate alkyl triflate[24] gave the corresponding ethers **18**−**21**. After adjusting the oxidation state at C7 at the aldehyde level,[25] the imidazole ring present in derivatives **3**−**6** was constructed according to van Leusen's method.[26] From **17**, the sequence could be modified to access the isomeric (6*R**,6a*S**)-ether **2**. Thus, treatment of **17** with $SOCl_2$ exchanged the 6-OH for a chlorine atom with retention of the relative stereochemistry. S_N2-type type displacement of the chlorine in **22** by sodium methoxide provided (6*R**,6a*S**)-ether **23**, which was then converted to **2** as described above.

Scheme 2 summarizes the synthesis of compounds **7**−**10**. From intermediates **16**, a Wittig reaction led to the exo-olefins **24**−**26**. The exomethylene derivative **24** was hydrogenated with diimide[27] to give **27** diastereoselectively (6*S**/6*R** = 90:10).[23] From **27**, formation of the imidazole **7** proceeded as described in Scheme 1. On the other hand, intermediates **25** and **26** were reduced under ionic conditions,[28] and the resulting esters (**28** and **29**, respectively) hydrolyzed to the corresponding acids **31** and **32** (6*S**/6*R** = 100:0). Reduction of the acids via their mixed anhydride, reoxidation of the alcohols to the aldehydes, and conversion to imidazole completed the synthesis of homologues **8** and **9**. Alternatively, cyclopropanation[29] of the double bond in **24** then imidazole formation yielded to spirocompound **10**. Enantiomers of compounds **1**, **3**, and **10** were separated by chromatography on chiral stationary phases.

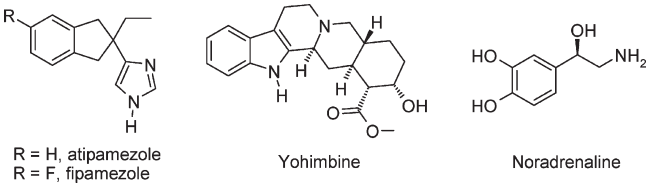

Figure 1. Selected α_2 ligands.

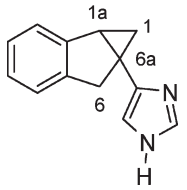

Figure 2. Structure of F 14805.

Table 1. In Vitro Affinity and Efficacy of Compounds **1**−**15** and Reference Agents

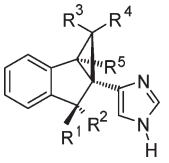

compd	R^1	R^2	R^3	R^4	R^5	affinity, pK_i[a] $h\alpha_{2A}$[b]	affinity, pK_i[a] $h\alpha_{1b}$[c]	$h\alpha_{2A}$ potency pK_B[d]
atipamezole						8.73 ± 0.09	5.71 ± 0.14	8.05 ± 0.28
fipamezole						8.14 ± 0.08	5.68 ± 0.06	7.84 ± 0.06
1	H	H	H	H	H	10.16 ± 0.07	8.88 ± 0.05	9.78 ± 0.43
(+)-**1**	H	H	H	H	H	10.10 ± 0.10	8.45 ± 0.01	9.64 ± 0.19
(−)-**1**	H	H	H	H	H	10.55 ± 0.14	8.98 ± 0.05	10.18 ± 0.22
2	H	OMe	H	H	H	7.93 ± 0.04	6.04 ± 0.10	6.90 ± 0.26
3	OMe	H	H	H	H	8.76 ± 0.02	6.99 ± 0.05	8.28 ± 0.07
(+)-**3**	OMe	H	H	H	H	9.25 ± 0.03	7.20 ± 0.01	8.54 ± 0.08
(−)-**3**	OMe	H	H	H	H	7.26 ± 0.02	5.75 ± 0.07	6.44 ± 0.06
4	OEt	H	H	H	H	8.48 ± 0.13	7.40 ± 0.27	8.36 ± 0.35
5	O*n*Pr	H	H	H	H	8.40 ± 0.11	7.94 ± 0.07	8.16 ± 0.07
6	O*i*Pr	H	H	H	H	7.34 ± 0.15	6.50 ± 0.01	6.88 ± 0.14
7	Me	H	H	H	H	9.66 ± 0.18	8.21 ± 0.15	9.54 ± 0.14
8	Et	H	H	H	H	9.29 ± 0.23	7.39 ± 0.24	8.91 ± 0.08
9	*n*Pr	H	H	H	H	9.07 ± 0.01	8.05 ± 0.04	8.70 ± 0.11
10	CH_2	CH_2	H	H	H	9.22 ± 0.17	7.83 ± 0.12	9.05 ± 0.02
(+)-**10**	CH_2	CH_2	H	H	H	9.48 ± 0.17	7.74 ± 0.20	8.88 ± 0.11
(−)-**10**	CH_2	CH_2	H	H	H	8.41 ± 0.14	7.01 ± 0.03	7.75 ± 0.23
11	H	H	H	Me	H	9.76 ± 0.22	7.48 ± 0.14	9.67 ± 0.02
12	H	H	H	Et	H	9.86 ± 0.10	7.78 ± 0.21	ND[e]
13	H	H	H	*n*Pr	H	9.39 ± 0.19	8.45 ± 0.30	9.24 ± 0.01
14	H	H	Me	Me	H	8.97 ± 0.18	6.75 ± 0.02	8.97 ± 0.34
15	H	H	H	H	Me	9.35 ± 0.16	7.40 ± 0.13	8.66 ± 0.04

[a] Binding affinity values are expressed as means ± SEM of at least two experiments, each performed in duplicate. [b] Affinity values were determined in C6 glial cells expressing $h\alpha_{2A}$ receptors. [c] Affinity values were determined in CHO cells stably expressing $h\alpha_{1b}$ receptors. [d] Potency of the antagonist that inhibits 50% of adrenaline-induced [^{35}S]GTPγS binding in CHO cells expressing $h\alpha_{2A}$ receptors. [e] Not determined.

Scheme 1. Synthesis of Compounds **2**−**6**

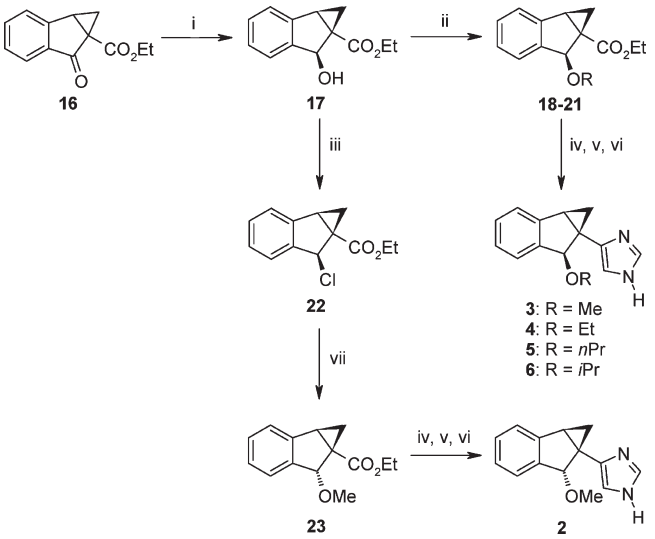

Reagents and conditions: (i) KBH_4, EtOH; (ii) ROTf, di-*t*BuPy, CH_2Cl_2; (iii) $SOCl_2$, $CHCl_3$; (iv) $LiBH_4$, THF; (v) $PySO_3$, NEt_3, DMSO; (vi) Tosmic, NH_3, MeOH; (vii) MeONa, MeOH.

Scheme 2. Synthesis of Compounds **7**−**10**

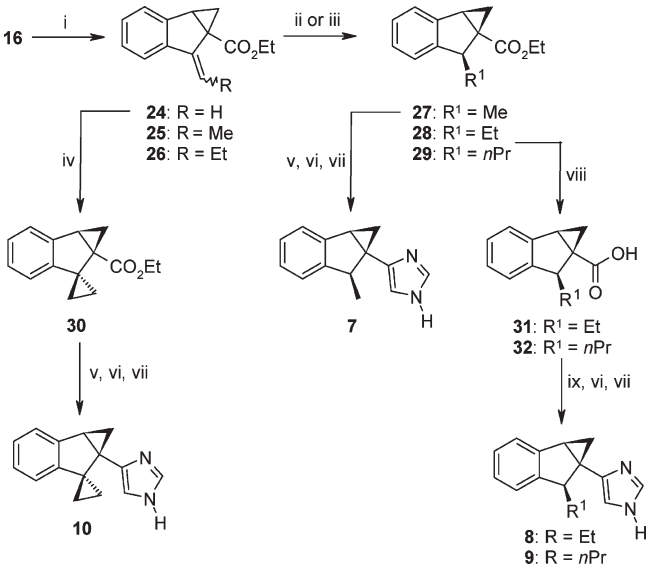

Reagents and conditions: (i) Ph_3PR^1Br, tBuOK or NaH; (ii) diimide, THF; (iii) Et_3SiH, TFA; (iv) ICH_2Cl, Et_2Zn; (v) $LiBH_4$, THF; (vi) $PySO_3$, NEt_3, DMSO; (vii) Tosmic, NH_3, MeOH; (viii) NaOH, EtOH; (ix) ClCOEt, NMM, $NaBH_4$, H_2O.

Results and Discussion

Most of the compounds reported here achieved subnanomolar affinity for the α_{2A} receptor (Table 1) but were not α_2 subtype selective (see Supporting Information). A substituent at C1, C1a, or C6 positions lowered affinity but augmented selectivity toward the α_{2A} receptor (vs α_{1b})[30] which reaches about 2 orders of magnitude in derivatives: **2**, (+)-**3**, **11**, **12**, **14**, and **15**. Upon incorporation of a *gem*-dimethyl group at C1, the α_{2A} affinity was spared whereas that at α_{1b} collapsed (**14** vs **1**). In contrast, a spiro-cyclopropane group at C6 has little influence on the compound affinity and selectivity (**10** vs **1**).

Conformational analysis carried out on neutral and protonated molecules **1**, **7**, **11**, and **15** showed that they share two sets of low-energy conformations in which the torsion angle about the C6a−C7 axis is near 80° or near 260°.[31] While the transition between these two local minima seems possible for molecules **1** and **7** (torsional energy barriers < 5 kcal/mol), it is thermodynamically disfavored in the cases of **11** and **15** (barriers > 10 kcal/mol). Grafting a substituent at C1 or C1a did therefore serve the objective of limiting the number of rotamers. In addition, the high α_{2A} affinity of **11** and **15** suggests that, in both cases, the conformational cost for binding is easily overcome. Accordingly, their bound state geometries should resemble that of the free molecules in their lowest energy conformations. Extrapolating these results to more flexible atipamezole-like molecules predicts that the imidazole and aromatic ring planes should adopt a quasi-orthogonal orientation upon binding to the α_{2A} receptor.

A substituent in the configuration 6*S** imposes no rotational constraint over the imidazole ring. 6*S**-Alkyl and -alkoxy groups were both tolerated even though the α_{2A} affinity of the corresponding ligands diminishes when the length of the 6*S**-chain is extended. On the other hand, an alkoxy group at C6 is reminiscent of the OH present in the endogenous agonist *R*-noradrenaline (Figure 1). The α_{2A} affinity of ethers is less than that of the corresponding alkyl derivatives, but only *S**-oriented (**3** vs **2**), linear O-radicals (**5** vs **6**) are accommodated. Further, the binding of **3** at the α_{2A} receptor shows a clear stereochemical preference as the affinity of (+)-**3** exceeds that of (−)-**3** by 2 orders of magnitude. We assumed that the oxygen atom in ethers participates in the binding interaction of **3**−**6** with the α_{2A} receptor. In contrast, a 6*S**-aliphatic group does not contribute to binding, as **7** and **10** are almost equipotent to **1** and only a 10-fold difference separates the affinity of (+)-**10** and (−)-**10**.

Whether compounds **1**−**10** occupy the same binding site on the protein is indeed uncertain. If so, 6*S**-ethers (**3**−**5**) and non-oxygenated ligands may position themselves differently inside it.

Next, the functional activity of the compounds at the hα_{2A} receptor was evaluated through a G-protein activation assay. None of the derivatives reported in Table 1 stimulated [^{35}S]GTPγS binding by itself (data not shown), indicating that they all lack agonist activity under the conditions of the assay. When tested against adrenaline-stimulated [^{35}S]GTPγS binding, they all inhibited nucleotide binding with pK_B values close to their pK_i (Table 1), demonstrating their potent antagonist properties at the α_{2A} receptor subtype.

In the subsequent phase, we assessed the central α_2 antagonist properties of the compounds in mice through their ability to counteract the hypothermia induced by the preferential α_{2A} receptor agonist guanabenz (Table 2).[32,33] Here, the ED_{50} value represents the dose of the compound necessary to significantly antagonize the hypothermia in 50% of guanabenz-treated animals. For each derivative, ED_{50} values were obtained for both the intraperitoneal (ip) and oral (po) routes of administration in order to estimate the compound bioavailability. All the derivatives in Table 2 but (−)-**10** were more potent than the reference agents irrespective of the route used. Thus, the oral potency of **1**, (+)-**3**, **4**, **5**, **7**−**9** exceeds that of fipamezole by at least 10-fold and only four derivatives i.e., (−)-**1**, (−)-**10**, **14**, and **15**, achieved a ratio po/ip greater than 4; fipamezole was indeed credited with improved pharmacokinetics over atipamezole.[34] Conversely, the antihypothermic effect of **4** and **5** was potentiated upon oral intake (po/ip < 0), suggesting that both compounds underwent some kind of presystemic metabolic activation. From a more general perspective, affinity at the α_{2A} receptor and potency to

Table 2. Guanabenz-Induced Hypothermia in Mice

	inhibition of hypothermia ED_{50} (mg/kg) [a]		
compd	ip [b]	po [b]	po/ip ratio
atipamezole	0.19 [0.12−0.29]	1.95 [0.92−4.13]	10.3
fipamezole	0.47 [0.16−1.42]	1.87 [0.62−5.67]	4.0
1	0.03 [0.008−0.13]	0.12 [0.02−0.90]	4.0
(+)-**1**	0.02 [0.005−0.07]	0.07 [0.02−0.29]	3.5
(−)-**1**	0.008 [0.001−0.06]	0.04 [0.01−0.14]	5.0
3	0.09 [0.04−0.20]	0.28 [0.11−0.72]	3.1
(+)-**3**	0.03 [0.004−0.23]	0.07 [0.02−0.29]	2.3
4	0.16 [0.05−0.54]	0.03 [0.007−0.11]	0.2
5	0.29 [0.12−0.73]	0.12 [0.02−0.90]	0.4
7	0.006 [0.002−0.02]	0.009 [0.0008−0.10]	1.5
8	0.03 [0.003−0.33]	0.04 [0.003−0.41]	1.3
9	0.10 [0.02−0.50]	0.12 [0.02−0.90]	1.2
10	0.06 [0.02−0.14]	0.22 [0.09−0.57]	3.7
(+)-**10**	0.08 [0.02−0.44]	0.22 [0.09−0.57]	2.8
(−)-**10**	0.18 [0.04−0.72]	1.87 [0.62−5.67]	10.4
11	0.06 [0.02−0.2]	0.19 [0.06−0.61]	3.2
13	0.10 [0.03−0.34]	0.33 [0.06−1.76]	3.3
14	0.07 [0.02−0.29]	0.47 [0.16−1.42]	6.7
15	0.06 [0.01−0.32]	0.66 [0.20−2.17]	11.0

[a] ED_{50} value represents the dose which produced an inhibitory effect in 50% of the guanabenz-treated animals, five animals tested per dose. [b] Values in brackets represent 95% confidence limits. Ip, intraperitoneal injection; po, oral gavage.

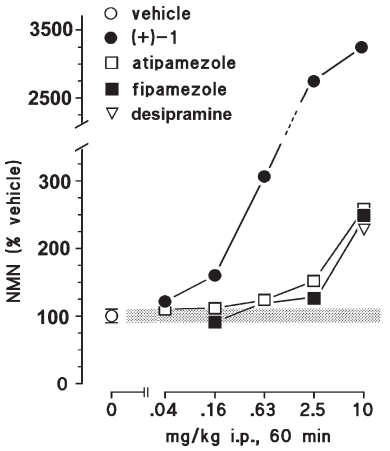

Figure 3. α2 antagonist induced increases in noradrenaline release (NMN levels) in mouse cortex in vivo: dose−response curves of (+)-**1** in comparison to atipamezole, fipamezole, and desipramine. Cortical NMN levels were measured in mice killed by head-focused microwave irradiation at 1 h after drug administrations by intraperitoneal (ip) injection. The effect of (+)-**1** was statistically significant ($P < 0.05$), in comparison to vehicle treated control animals, at doses ≥0.16 mg/kg. The effects of atipamezole, fipamezole, and desipramine were significant at doses ≥0.63 mg/kg.

antagonize guanabenz-induced hypothermia (ip) tended to vary in the same direction for racemates listed in Table 2.

As mentioned above, mouse thermoregulation provides a readily accessible index of central α_{2A} antagonist activity. One limitation, however, comes from the fact that it reflects the competition between the ligand and the exogenous agonist guanabenz at postjunctional α_{2A} heteroreceptors in the hypothalamus rather than that between the ligand and endogenous NA at $\alpha_{2A/C}$ autoreceptors in the LC.[2] As a more relevant approach to the targeted mechanism (i.e., presynaptic regulation of noradrenergic transmission), we explored the NA-releasing potential of the products in mice frontal cortex, a brain region that receives noradrenergic projections directly from the LC. To this end, we measured the levels of normetanephrine (NMN), a metabolite formed exclusively from NA[35] in the extracellular space. Figure 3 depicts the increase in cortical NMN relative to control animals following the ip injection of (+)-**1**, atipamezole, and fipamezole. For intermechanism comparison, we also include the response elicited by 10 mg/kg of the selective NA reuptake inhibitor desipramine.[36] Compound (+)-**1**, from 0.16 to 10 mg/kg, dose-dependently enhanced cortical NMN levels by up to 3096 ± 301%. Remarkably, the amplitude of the effect evoked by 0.3 mg/kg of (+)-**1** turns out to be equivalent to that produced by 10 mg/kg of atipamezole, fipamezole, or desipramine (i.e., 258 ± 37, 247 ± 15, and 223 ± 10%, respectively). Compounds (+)-**1** is therefore more potent (>30-fold) and more efficacious (>10-fold) than benchmarks at modulating NA turnover, at least after acute administration.[36,37] Given the role of NA transmission in cognition and other physiological processes,[38] we believe that the field would benefit from ligands able to make the synaptic concentrations of tonic NA to vary over a much wider range.[39] Although the precise mechanism by which (+)-**1** controls NA outflow has not been elucidated yet, it appears unlikely that it involves the sole blockade of presynaptic $\alpha_{2A/C}$ receptors.[40]

In any case, neurochemical as well as temperature regulation data point to (+)-**1** as being a potent, centrally active α_2 antagonist. Particularly remarkable is the capacity of (+)-**1** at boosting cortical NA release. From a medicinal chemistry perspective, the finding that restricting the conformational freedom of atipamezole undermines selectivity (α_2 vs α_1) is somewhat perplexing.[41]

In light of the massive NA discharge generated by (+)-**1**, its impact on cardiovascular function became important to address, bearing in mind that the targeted patients would be aged and may have a compromised cardiovascular system.

In intact rat, the cardiovascular effects of (+)-**1** result from its action at α adrenergic receptors[42] within the sympathetic nervous system, the heart, and the vasculature.[43] The interplay between these mechanisms complicates the interpretation of data tremendously. Things are simpler in the pithed rat where the cardiovascular effects can be dissociated from any modulatory control by the CNS.[44a] In such a model, intravenous administration of (+)-**1** caused a dose related pressor response from 0.63 μg/kg upward (Figure 4). This rise in diastolic arterial blood pressure (DAP) may be due to activation of α_1 and/or α_2 receptors located in the myocardia and/or the blood vessel walls (i.e., smooth muscle, endothelium, and nerve endings).[43,44b] As a first step toward identification of the receptor(s) at the origin of this hypertensive effect, we challenged the DAP produced by (+)-**1** at a dose of 2.5 μg/kg (iv) with selective α-adrenergic antagonists (Figure 5). Thus, (+)-**1** elevated DAP (42 ± 13 mmHg) relative to baseline, and this effect was reversed by the nonsubtype selective α_2 antagonist rauwolscine[45] (0.63 mg/kg, iv), while it was not significantly affected by the α_1 antagonist prazosin[46] (0.16 mg/kg, iv). The hypertension that developed upon administration of (+)-**1** is therefore mostly driven by activation of vascular α_2 receptors,[44b] although a minor contribution of α_1 receptors cannot be ruled out (see Supporting Information). This finding is regarded as important, for it reveals that (+)-**1** activates peripheral α_2 receptors. Functional activity results (cf. Table 1) indicate, however, that this agonist-type response is more likely conveyed by α_{2B} and/or α_{2C} receptors.

In the anesthetized rat, the dose−response curve produced by iv injection of (+)-**1** was shifted rightward and its slope was

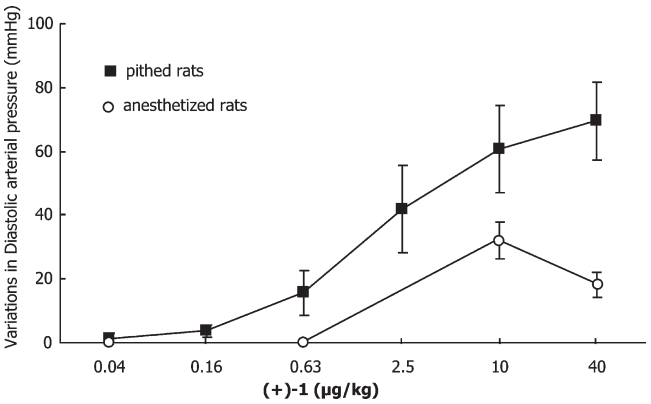

Figure 4. Variations in diastolic arterial pressure measured immediately after intravenous injection of (+)-**1**. Filled squares: (+)-**1** administered in the pithed rat. Open circles: (+)-**1** administered in the anesthetized, normotensive rat.

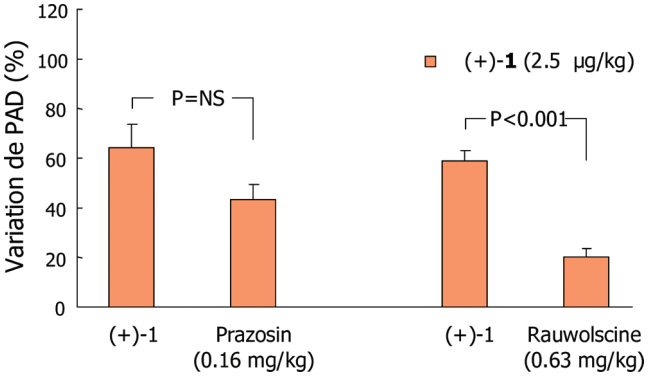

Figure 5. Effects of the prototypical α_1-antagonist prazosin and α_2-antagonist rauwolscine on the pressor response elicited by iv injection of (+)-**1** in the pithed rat. Prazosin or rauwolscine were both given by iv injection 15 min before (+)-**1**. NS, not significant ($P > 0.05$).

shallower than that observed in the pithed rat (Figure 4). DAP remained unchanged up to 0.16 μg/kg. Beyond that dose, (+)-**1** evoked a transient (<1 min) and slight increase in DAP that was maximal at 10 μg/kg (26 ± 6 mmHg) and thereafter began to decrease. The initial pressor response was accompanied by a brief (<1 min) reflex bradycardia. Interestingly, heart rate and DAP rapidly returned to basal values after (+)-**1** administration.

Thus, the sustained, pronounced hypertensive effect observed with (+)-**1** in the absence of CNS input (pithed rat) is attenuated and of shorter duration (in intact rat),[47] an observation consistent with (+)-**1** exerting offsetting actions at central and peripheral α_2 receptors.

Conclusions

We describe a novel series of conformationally constrained analogues of atipamezole. Most compounds have high affinity for but bind indiscriminately to α_2 receptor subtypes. They exhibited a good degree of selectivity for α_2 receptors (versus α_{1b}) and showed potent α_{2A} antagonist activity in a functional [^{35}S]GTPγS-based assay. These ligands were all centrally active following oral administration. Among the structural modifications implemented, incorporation of a methyl at C1 or C6a position hindered rotation about the C6a-imidazole bond, a characteristic that we used to get structural information about the antagonist bound conformations of atipamezole-like molecules at the α_{2A} receptors.

Further characterization performed on a representative member of the series, (+)-**1**, uncovered several intriguing features. Thus, studies in mice confirmed that (+)-**1** behaves as a potent antagonist on presynaptic $\alpha_{2A/C}$ receptors in the LC and highlighted its outstanding efficacy at triggering cortical NA release after acute, systemic administration.

On the cardiovascular side, (+)-**1** substantially increases blood pressure in the pithed rat and this effect was shown to be primarily mediated by stimulation of vascular α_2 receptors. The pressor response induced by (+)-**1** was, however, much reduced and of shorter duration in the intact, anesthetized rats, suggesting that its central and peripheral actions oppose each other.

Merging central $\alpha_{2A/C}$ antagonism with a non-α_2 mechanism that amplifies NA release in LC projection areas should reduce dosing of the compound and, thereby, minimize its off-target effects. Additionally, agonism at peripheral α_2 receptors might temper its cardiovascular impact. As far as CNS interventions are concerned, we believe that there is still room for improving the benefit-risk profile of α_2 ligands.

Experimental Section

Chemistry. Melting points were determined on a Büchi 530 melting point apparatus and were not corrected. ^{1}H NMR spectra were recorded on a Bruker Avance 400 spectrometer operating at 400 MHz for ^{1}H and 100 MHz for ^{13}C. Chemical shifts are reported in δ value (ppm) relative to an internal standard of tetramethylsilane. Infrared (IR) spectra were obtained on a Nicolet FT 510 P spectrophotometer. Microanalyses were obtained on a Fison EA 1108/CHN analyzer. Mass spectra (TSQ 7000 Finnigan, Thermoelectron Corporation) were determined by atmospheric pressure chemical ionization (APCI, MeOH/H_2O/AcOH, 50:50:1), and only 100% relative intensity peaks are given. Analytical thin-layer chromatography was carried out on precoated plates (silica gel, 60 F 254 Merck). Optical rotations were measured on a Perkin-Elmer 241 model polarimeter. The purity of final compounds was established by HPLC using Xbridge 8.5 μm, 4.6 mm × 250 mm reverse phase column at a flow rate of 1 mL/min (eluting with $CH_3CN/H_2O/KH_2PO_4$, 200:800:6.8 g). The compounds were detected at 220 nm. The purity of final products was ≥95% unless otherwise noted.

General Method for the Preparation of Imidazoles 2−10. To a solution of the 1a,6-dihydro-1*H*-cyclopropa[a]inden-6a-yl)-1*H*-carboxaldehyde (1 equiv) in EtOH (15 mL/g) was added successively *p*-toluenesulfonylmethyl isocyanide (1 equiv) and NaCN (0.1 equiv). This solution was stirred for 1 h at room temperature and then concentrated in vacuo. The residue was taken up in a solution of ammonia in MeOH (5N, 10 equiv) and heated at 90 °C for 16 h in sealed flask. The cooled reaction mixture was concentrated in vacuo and the residue taken up in ethyl acetate. The precipitate formed was filtered out and the solid washed with ethyl acetate. The combined organic phase was concentrated in vacuo, the residue taken up in diethyl ether and extracted with HCl (1N). The combined aqueous acid phase was neutralized NaOH (10N), extracted with ethyl acetate, and then the combined organic phase washed with brine, dried over Na_2SO_4, filtered, and concentrated in vacuo.

4-(1a,6-Dihydro-1*H*-cyclopropa[a]inden-6a-yl)-1*H*-imidazole (1). Purification by chromatography on neutral alumina eluting with chloroform gave **1** (43%).The fumarate salt of **1** gave a white powder mp = 152 °C. IR (KBr): 3001, 1618, 757 ν cm^{-1}. ^{1}H NMR (DMSO-d_6) δ 0.50 (t, J = 4.0 Hz, 1H), 1.71 (q, J = 4.0 Hz, 1H), 2.53 (m, 1H), 3.18 (d, J = 17.2 Hz, 1H), 3.48 (d, J = 17.2 Hz, 1H), 6.62 (s, 2H), 6.99 (s, 1H), 7.06−7.11 (m, 2H),

7.19−7.21 (m, 1H), 7.27−7.29 (m, 1H), 7.65 (s, 1H). ^{13}C NMR (DMSO-d_6) δ 23.6 (CH), 25.6 (C), 32.8 (CH2), 39.6 (CH2), 116.0 (CH), 122.8 (CH), 125.1 (CH), 125.3 (CH), 125.8 (CH), 133.9 (CH), 134.6 (CH), 136.0 (C), 141.3 (C), 146.1 (C), 165.9 (C). MS: m/z = 197 [MH$^+$]. Anal. ($C_{13}H_{12}N_2 \cdot C_4H_4O_4$) C, H, N.

(+)-4-(1a,6-Dihydro-1*H*-cyclopropa[a]inden-6a-yl)-1*H*-imidazole, (+)-1. $[\alpha]_D^{25}$ +108.5° (c 0.32, CH_3OH). HPLC: ChiralpackAD (Daicel), eluting with hexane/EtOH, 90:10, t_R 7.58 min, purity 99.97%. Anal. ($C_{13}H_{12}N_2.C_4H_4O_4$) C, H, N.

(−)-4-(1a,6-Dihydro-1*H*-cyclopropa[a]inden-6a-yl)-1*H*-imidazole, (−)-1. $[\alpha]_D^{25}$ −106.2° (c 0.35, CH_3OH). HPLC: ChiralpackAD (Daicel), eluting with hexane/EtOH, 90:10, t_R 11.17 min, purity 99.49%. Anal. ($C_{13}H_{12}N_2 \cdot C_4H_4O_4$) C, H, N.

(6*R,6a*S**)-4-(6-Methoxy-1a,6-dihydro-1*H*-cyclopropa[a]-inden-6a-yl)-1*H*-imidazole (2).** Purification by silica gel chromatography eluting with dichloromethane/methanol (95:5) gave **2** (44%). The maleate salt of **2** gave a white powder mp = 158 °C. IR (KBr): 3180, 2360, 1570, 1460, 874 ν cm^{-1}. ^{1}H NMR (DMSO-d_6) δ 0.61 (t, J = 4.0 Hz, 1H), 1.59 (q, J = 4.0 Hz, 1H), 2.97 (m, 1H), 3.13 (s, 3H), 4.86 (d, J = 1.2 Hz, 1H), 6.04 (s, 2H), 6.99 (s, 1H), 7.22 (t, J = 6.4 Hz, 1H), 7.29 (t, J = 6.4 Hz, 1H), 7.42 (d, J = 7.2 Hz, 1H), 7.47 (d, J = 7.2 Hz, 1H), 7.59 (d, J = 1.2 Hz, 1H), 8.89 (d, J = 1.2 Hz, 1H). ^{13}C NMR (DMSO-d_6) δ 27.3 (CH_2), 28.9 (CH), 29.6 (C), 55.9 (CH_3), 83.9 (CH), 117.6 (CH), 123.0 (CH), 125.9 (CH), 126.5 (CH), 128.5 (CH), 131.7 (C), 133.9 (CH), 135.4 (CH), 140.0 (C), 145.5 (C), 167.0 (C). MS: m/z = 227 [MH$^+$], 195 [−MeOH]. Anal. ($C_{14}H_{14}N_2O \cdot C_4H_4O_4$) C, H, N.

(6*S,6a*S**)-4-(6-Methoxy-1a,6-dihydro-1*H*-cyclopropa[a]-inden-6a-yl)-1*H*-imidazole (3).** Purification by silica gel chromatography eluting with dichloromethane/methanol (95:5) gave **3** (45%). The fumarate salt of **3** gave a white powder mp = 122 °C. IR (KBr): 3138, 2826, 1685, 975 ν cm^{-1}. ^{1}H NMR (DMSO-d_6) δ 0.97 (t, J = 4.0 Hz, 1H), 1.63 (q, J = 4.0 Hz, 1H), 2.44 (q, J = 4.0 Hz, 1H), 3.40 (s, 3H), 5.53 (s, 1H), 6.62 (s, 2H), 7.10−7.24 (m, 5H), 7.63 (s, 1H). ^{13}C NMR (DMSO-d_6) δ 22.5 (CH_2), 27.8 (C), 32.7 (CH), 56.8 (CH_3), 86.5 (CH), 114.3 (CH), 123.0 (CH), 125.8 (CH), 126.0 (CH), 127.8 (CH), 133.9 (CH), 134.7 (CH), 140.0 (C), 141.6 (C), 145.2 (C), 166.0 (C). MS: m/z = 227 [MH$^+$], 195 [−MeOH]; Anal. ($C_{14}H_{14}N_2O \cdot C_4H_4O_4$) C, H, N.

(+)-4-(6-Methoxy-1a,6-dihydro-1*H*-cyclopropa[a]inden-6a-yl)-1*H*-imidazole, (+)-3. $[\alpha]_D^{25}$ +106.8° (c 0.34, CH_3OH). HPLC: ChiralpackAD (Daicel), eluting with hexane/EtOH, 90:10, t_R 8.37 min, purity 100.0%. Anal. ($C_{14}H_{14}N_2O \cdot C_4H_4O_4$) C, H, N.

(−)-4-(6-Methoxy-1a,6-dihydro-1*H*-cyclopropa[a]inden-6a-yl)-1*H*-imidazole, (−)-3. $[\alpha]_D^{25}$ −107.9° (c 0.36, CH_3OH). HPLC: ChiralpackAD (Daicel), eluting with hexane/EtOH, 90:10, t_R 10.89 min, purity 99.39%. Anal. ($C_{14}H_{14}N_2O \cdot C_4H_4O_4$) C, H, N.

(6*S,6a*S**)-4-(6-Ethoxy-1a,6-dihydro-1*H*-cyclopropa[a]inden-6a-yl)-1*H*-imidazole (4).** Purification by silica gel chromatography eluting with dichloromethane/methanol (97:3) gave **4** (53%). The fumarate salt of **4** gave a white powder mp = 158 °C. IR (KBr): 3081, 2829, 1612, 1078, 983 ν cm^{-1}. ^{1}H NMR (DMSO-d_6) δ 0.98 (t, J = 4.0 Hz, 1H), 1.11 (t, J = 6.8 Hz, 3H), 1.67 (q, J = 4.0 Hz, 1H), 2.41 (q, J = 4.0 Hz, 1H), 3.58 (m, J = 6.8 Hz, 1H), 3.70 (m, J = 6.8 Hz, 1H), 5.62 (s, 1H), 6.62 (s, 2H), 7.06 (d, J = 1.2 Hz, 1H), 7.11−7.23 (m, 4H), 7.61 (d, J = 1.2 Hz, 1H). ^{13}C NMR (DMSO-d_6) δ 15.5 (CH_3), 22.3 (CH_2), 27.9 (C), 32.7 (CH), 64.2 (CH_2), 84.9 (CH), 114.0 (CH), 123.0 (CH), 125.8 (CH), 126.0 (CH), 127.7 (CH), 133.9 (CH), 134.7 (CH), 140.0 (C), 141.9 (C), 145.2 (C), 166.0 (C). MS: m/z = 241 [MH$^+$], 195 [−EtOH]. Anal. ($C_{15}H_{16}N_2O \cdot C_4H_4O_4$) C, H, N.

(6*S,6a*S**)-4-(6-Propyloxy-1a,6-dihydro-1*H*-cyclopropa[a]-inden-6a-yl)-1*H*-imidazole (5).** Purification by silica gel chromatography eluting with dichloromethane/methanol (90:10) gave **5** (31%). The fumarate salt of **5** gave a white powder mp = 114 °C. IR (KBr): 3139, 2963, 2852, 1685, 1085, 974 ν cm^{-1}. ^{1}H NMR (DMSO-d_6) δ 0.86 (t, J = 7.2 Hz, 3H), 0.98 (t, J = 4.0 Hz, 1H), 1.49 (m, J = 7.2 Hz, 2H), 1.66 (q, J = 4.0 Hz, 1H), 2.41 (q, J = 4.0 Hz, 1H), 3.50 (m, J = 6.4 Hz, 1H), 3.61 (m, J = 6.4 Hz, 1H), 5.61 (s, 1H), 6.62 (s, 2H), 7.05 (s, 1H), 7.12−7.23 (m, 4H), 7.58 (s, 1H). ^{13}C NMR (DMSO-d_6) δ 10.6 (CH_3), 22.3 (CH_2), 22.7 (CH_2), 27.9 (C), 32.7 (CH), 70.4 (CH_2), 85.0 (CH), 114.5 (CH), 123.0 (CH), 125.8 (CH), 125.9 (CH), 127.7 (CH), 133.9 (CH), 134.7 (CH), 139.0 (C), 141.9 (C), 145.2 (C), 166.0 (C). MS: m/z = 255 [MH$^+$], 195 [−nPrOH]. Anal. ($C_{16}H_{18}N_2O \cdot C_4H_4O_4$) C, H, N.

(6*S,6a*S**)-4-(6-Isopropyloxy-1a,6-dihydro-1*H*-cyclopropa[a]-inden-6a-yl)-1*H*-imidazole (6).** Purification by silica gel chromatography eluting with dichloromethane/methanol (95:5) gave **6** (27%). The fumarate salt of **6** gave a white powder mp = 175 °C. IR (KBr): 3109, 2974, 1701, 1374, 1059, 743 ν cm^{-1}. ^{1}H NMR (DMSO-d_6) δ 0.96 (t, J = 4.0 Hz, 1H), 1.03 (d, J = 6.4 Hz, 3H), 1.14 (d, J = 6.4 Hz, 3H), 1.64 (q, J = 4.0 Hz, 1H), 2.36 (q, J = 4.0 Hz, 1H), 3.93 (m, J = 6.4 Hz, 1H), 5.73 (s, 1H), 6.62 (s, 2H), 7.04 (s, 1H), 7.12−7.22 (m, 4H), 7.65 (s, 1H). ^{13}C NMR (DMSO-d_6) δ 21.8 (CH_3), 21.9 (CH_3), 23.5 (CH_2), 27.9 (C), 32.7 (CH), 69.3 (CH), 82.8 (CH), 114.4 (CH), 122.9 (CH), 125.7 (CH), 125.8 (CH), 127.5 (CH), 133.9 (CH), 134.8 (CH), 139.6 (C), 142.4 (C), 145.1 (C), 166.0 (C). MS: m/z = 255 [MH$^+$], 195 [−iPrOH]. Anal. ($C_{16}H_{18}N_2O \cdot C_4H_4O_4$) C, H, N.

(6*S,6a*R**)-4-(6-Methyl-1a,6-dihydro-1*H*-cyclopropa[a]-inden-6a-yl)-1*H*-imidazole (7).** Purification by silica gel chromatography eluting with dichloromethane/methanol (90:10) gave **7** (55%). The fumarate salt of **7** gave a white powder mp = 167 °C. IR (KBr): 2869, 2825, 1618, 759 ν cm^{-1}. ^{1}H NMR (DMSO-d_6) δ 0.43 (t, J = 4.0 Hz, 1H), 1.30 (d, J = 7.2 Hz, 3H), 1.51 (q, J = 4.0 Hz, 1H), 2.52 (q, J = 4.0 Hz, 1H), 3.81 (q, J = 7.0 Hz, 1H), 6.62 (s, 2H), 7.01 (s, 1H), 7.07−7.16 (m, 3H), 7.24 (m, 1H), 7.67 (s, 1H). ^{13}C NMR (DMSO-d_6) δ 16.2 (CH_3), 20.3 (CH_2), 29.9 (C), 31.8 (CH), 43.1 (CH), 114.9 (CH), 122.8 (CH), 124.3 (CH), 125.4 (CH), 125.9 (CH), 134.0 (CH), 134.7 (CH), 139.1 (C), 145.7 (C), 145.9 (C), 166.1 (C). MS: m/z = 211 [MH$^+$]. Anal. ($C_{14}H_{14}N_2 \cdot C_4H_4O_4$) C, H, N.

(6*S,6a*R**)-4-(6-Ethyl-1a,6-dihydro-1*H*-cyclopropa[a]inden-6a-yl)-1*H*-imidazole (8).** Purification by silica gel chromatography eluting with dichloromethane/methanol (96:4) gave **8** (30%). The fumarate salt of **8** gave a white powder mp = 159 °C. IR (KBr): 3147, 2950, 1628 ν cm^{-1}. ^{1}H NMR (DMSO-d_6) δ 0.57 (t, J = 4.0 Hz, 1H), 0.99 (t, J = 7.6 Hz, 3H), 1.47 (m, J = 7.2 Hz, 1H), 1.67 (q, J = 4.0 Hz, 1H), 1.91 (m, J = 7.2 Hz, 1H), 2.35 (q, J = 4.0 Hz, 1H), 3.76 (q, J = 5.2 Hz, 1H), 6.62 (s, 2H), 6.98 (s, 1H), 7.08−7.12 (m, 2H), 7.18 (t, J = 3.6 Hz, 1H), 7.22−7.24 (m, 1H), 7.63 (s, 1H). ^{13}C NMR (DMSO-d_6) δ 12.8 (CH_3), 19.2 (CH_2), 26.0 (CH_2), 29.3 (C), 32.7 (CH), 49.6 (CH), 115.0 (CH), 122.9 (CH), 124.5 (CH), 125.4 (CH), 125.9 (CH), 134.0 (CH), 134.5 (CH), 140.0 (C), 145.5 (C), 145.8 (C), 166.1 (C). MS: m/z = 225 [MH$^+$]. Anal. ($C_{15}H_{16}N_2 \cdot C_4H_4O_4$) C, H, N.

(6*S,6a*R**)-4-(6-Propyl-1a,6-dihydro-1*H*-cyclopropa[a]inden-6a-yl)-1*H*-imidazole (9).** Purification by silica gel chromatography eluting with dichloromethane/methanol (97:3) gave **9** (24%). The maleate salt of **9** gave a white powder mp = 150 °C. IR (KBr): 3109, 2957, 1624, 1491, 860 ν cm^{-1}. ^{1}H NMR (DMSO-d_6) δ 0.72 (t, J = 4.0 Hz, 1H), 0.85 (t, J = 7.2 Hz, 3H), 1.35−1.47 (m, 3H), 1.74 (q, J = 5.2 Hz, 1H), 1.86 (m, 1H), 2.56 (q, J = 4.0 Hz, 1H), 3.85 (q, J = 4.8 Hz, 1H), 6.05 (s, 2H), 7.14−7.21 (m, 3H), 7.27−729 (m, 1H), 7.55 (s, 1H), 8.82 (s, 1H). ^{13}C NMR (DMSO-d_6) δ 14.1 (CH3), 18.5 (CH_2), 20.6 (CH_2), 26.9 (C), 32.7 (CH), 35.1 (CH_2), 48.4 (CH), 115.7 (CH), 123.1 (CH), 124.6 (CH), 125.9 (CH), 126.3 (CH), 134.0 (CH), 135.2 (CH), 136.9 (C), 144.5 (C), 144.9 (C), 167.0 (C). m/z = 239 [MH$^+$]. Anal. ($C_{16}H_{18}N_2 \cdot C_4H_4O_4$) C, H, N.

4-(6-Spirocyclopropyl-1a,6-dihydro-1*H*-cyclopropa[a]inden-6a-yl)-1*H*-imidazole (10). Purification by silica gel chromatography eluting with dichloromethane/methanol (96:4) gave **10** (30%). The fumarate salt of **10** gave a white powder mp = 220 °C. IR (KBr): 3132, 2821, 1654, 1623, 845, 759 ν cm^{-1}. ^{1}H NMR (DMSO-d_6) δ 0.60 (t, J = 4.0 Hz, 1H), 0.77−0.84 (m, 2H),

0.93−0.98 (m, 1H), 1.06−1.11 (m, 1H), 1.45 (q, J = 4.0 Hz, 1H), 2.71 (q, J = 4.0 Hz, 1H), 6.62 (s, 2H), 6.67 (m, 1H), 6.90 (s, 1H), 7.06 (m, 2H), 7.29 (m, 1H), 7.63 (s, 1H). ^{13}C NMR (DMSO-d_6) δ 12.9 (CH2), 17.0 (CH2), 24.0 (CH_2), 29.8 (C), 30.0 (CH), 32.5 (C), 119.3 (CH), 122.6 (CH), 125.2 (CH), 125.6 (CH), 134.0 (CH), 135.0 (CH), 144.9 (C), 146.9 (C), 166.0 (C). m/z = 223 [MH^+]. Anal. ($C_{15}H_{14}N_2 \cdot C_4H_4O_4$) C, H, N.

(+)-4-(6-Spirocyclopropyl-1a,6-dihydro-1*H*-cyclopropa[a]-inden-6a-yl)-1*H*-imidazole, (+)-10. $[\alpha]_D^{25}$ +50.5° (c 0.33, CH_3OH). HPLC: Chiralcel OD (Daicel), eluting with hexane/EtOH, 95:5, t_R 19.32 min, purity 99.94%. Anal. ($C_{15}H_{14}N_2 \cdot C_4H_4O_4$) C, H, N.

(−)-4-(6-Spirocyclopropyl-1a,6-dihydro-1*H*-cyclopropa[a]-inden-6a-yl)-1*H*-imidazole, (−)-10. $[\alpha]_D^{25}$ −47.7° (c 0.29, CH_3OH). HPLC: Chiralcel OD (Daicel), eluting with hexane/EtOH, 95:5, t_R 14.6 min, purity 99.60%. Anal. ($C_{15}H_{14}N_2 \cdot C_4H_4O_4$) C, H, N.

Biology. Animals were housed and tested in an Association for the Assessment and Accreditation of Laboratory Animal Care (AAALAC)-accredited facility in strict compliance with all applicable regulations, and the protocol was carried out in compliance with French regulations and institutional Ethical Committee guidelines for animal research. Atipamezole[48] and fipamezole[49] were prepared according to literature procedures. Guanabenz acetate (lot CC-591 A) was purchased from Research Biochemicals Inc.

Competition Binding at α_2 and α_{1b} Adrenergic Receptors. Competition binding assays at C6 glial cells stably expressing human (h)α_{2A}, hα_{2B}, or hα_{2C} adrenergic receptors or at CHO cells stably expressing hα_{1b} receptors were performed as previously described.[50] Briefly, C6-hα_2 or CHO-hα_{1b} membranes (10−20 μg of protein) were resuspended in 50 mM Tris buffer, pH 7.6, and incubated for 120 min at 25 °C with the radioligands, [^{3}H]-RX821002 for hα_2 (GE Healthcare Europe GmbH, Orsay, France; concentrations about 2, 10, and 4 nmol for hα_{2A}, hα_{2B}, or hα_{2C} adrenergic receptors, respectively) or [^{3}H]-prazosin for hα_{1B} receptors (GE Healthcare; concentration about 0.2 nmol) and test compounds in a final volume of 0.5 mL. Nonspecific binding was defined with phentolamine (10 μmol). Incubations were terminated by rapid filtration through 0.1% polyethylenimine-presoaked Whatman GF/B filters using a 96 well filtermate harvester (PerkinElmer Life Science, Boston, MA). Radioactivity retained on the filters was determined by liquid scintillation counting using a Top-Count microplate scintillation counter (PerkinElmer Life Science).

G Protein Activation. hα_{2A} receptor-linked G protein activation was determined by measuring the stimulation of [^{35}S]-GTPγS (>1000 Ci/mM; GE Healthcare Europe GmbH, Orsay, France) binding at membranes of CHO-hα_{2A} cells. Briefly, membranes were preincubated 30 min at 30 °C with compounds alone or with adrenaline (antagonist experiments) in a buffer containing 20 mM HEPES, 0.3 μM GDP, 3 mM $MgCl_2$, 100 mM NaCl, pH 7.4. The reaction was started by addition of 0.50 nmol [^{35}S]GTPγS in a final volume of 0.5 mL, and incubation was performed for an additional 30 min. Experiments were terminated by rapid filtration, and radioactivity retained on the filters was determined by liquid scintillation counting using a TopCount microplate scintillation counter. Basal binding is defined as 0%, whereas adrenaline (10 μmol)-stimulated [^{35}S]GTPγS binding performed in each experiment is defined as 100%.

Data Analysis. Isotherms were analyzed by nonlinear regression using the program Prism (GraphPad Software, San Diego, CA) to yield IC_{50} values. In binding experiments, inhibition constants (K_i) were derived from IC_{50} values according to the Cheng−Prusoff equation: $K_i = IC_{50}/(1 + L/K_d)$, where L is the concentration of [^{3}H]-radioligand and K_d is its dissociation constant at the respective α-adrenergic receptor subtype. K_B values for antagonism of adrenaline-stimulated [^{35}S]GTPγS incorporation were calculated from IC_{50} values as follows: $K_B = IC_{50}/(1 + [Ago]/EC_{50\text{-}Ago})$, where Ago is the concentration of adrenaline (1 μM) and $EC_{50\text{-}Ago}$ is the EC_{50} of adrenaline for stimulation of [^{35}S]GTPγS binding at hα_{2A} receptors. All values are expressed as mean ± SEM of at least two experiments, each performed in duplicate.

Guanabenz-Induced Hypothermia in Mice. Male NMRI mice (Iffa Credo, France) weighing 30−32 g were housed in groups of 15 with free access to food and water. There was a 12 h/12 h light/dark cycle. Rectal temperature was measured to the nearest 0.1 °C by insertion of a thermistor probe (Ellab, type DM 852) approximately 1.5 cm into the rectum for 3−5 s until a stable temperature reading was obtained. Mice were given vehicle or drug via either the intraperitoneal (10 mL/kg injection volume) or oral route. Drugs were dissolved in distilled water. Five min after ip injection or 35 min after po administration, animals received an ip injection of 1 mg/kg of guanabenz. The rectal temperature was measured 25 min after the administration of guanabenz. The total number of animals tested per dose was five.

Results were expressed as the mean ± SEM of rectal temperature and were analyzed by one-way analysis of variance, with drug treatment as the factor, followed by a 2-tailed Student t test (GB-STAT, Friedman, 1991). For each drug dose group, the inhibition of hypothermia induced by guanabenz was also expressed as percentage of inhibition according to the following formula: $[(X - G)/(V - G)] \times 100$, where X represents the rectal temperature of mice treated by guanabenz + the compound being studied, G represents the rectal temperature of mice treated by guanabenz + vehicle, and V represents the rectal temperature of control mice treated by vehicle + vehicle. The percentages of inhibition of mice treated by guanabenz + vehicle and of control mice were 0 and 100%, respectively. The inhibitory potency of each test drug was estimated by an ED_{50} value, representing the dose which produced an inhibitory effect in 50% of the animals. ED_{50} values and their 95% confidence limits were obtained by means of the method of Litchfield and Wilcoxon[51] (1949) using the PHARM/PCS program no. 46 of Tallarida and Murray (1987).[52]

Cortical Normetanephrine (NMN) Levels in Mice. Test substances were dissolved by vortexing and bath sonication in filtered deionized water (Direct-Q) containing Tween (1 drop in 10 mL water), diluted serially in filtered deionized water, and administered by the intraperitoneal route to male albino mice (IFFA NMRI [IOPS]) at the doses indicated (10 mL/kg injection volume). Animals were killed 1 h later by head-focused microwave irradiation (3.8 kW, 2450 MHz, 0.9 s; Sacron model 8000, SAIREM, Vaulx-en-Velin, France).[35a] Frontal cortices were dissected from the brain, and the levels of NMN in perchloric acid extracts of tissue samples were quantified using HPLC with electrochemical detection, as previously described.[35b] NMN levels in drug-treated groups are expressed as a percentage of the levels in the vehicle control group. Differences (P values) between drug-treated groups and the saline control group were determined by Kruskal−Wallis ANOVA + Mann−Whitney U-test.

Cardiovascular Profiles in Rats. Male OFA (SD) rats (Iffa Credo, France) weighing 280−300 g were housed with free access to food and water. There was a 12 h/12 h light/dark cycle.

Pithed Rats. Animals (n = 6) were anesthetized with isofluorane 2% and then the brain destroyed by a steel rod which was inserted into the spinal cord. Rats were mechanically ventilated (60 cycles/min; 2.5 mL/cycle, Harvard apparatus South Natick, MA) in order to maintain blood gases within the physiological range. Rectal temperature was maintained at 37 °C by means of a rectal probe thermometer attached to a homeothermic blanket control unit (Harvard). Bilateral vagotomy was performed, and atropine sulfate (1.25 mg/kg) was administered iv. Catheters were inserted into the penile vein for infusing drugs and into the right carotid artery to continuously measure arterial pressure via a Statham P10EZ pressure transducer (Viggo-Spectramed, Oxnad, CA) connected to a Gould amplifier (Gould Instruments, France). Heart rate (HR) was derived from arterial pressure signal by means of a Biotach tachometer (Gould

Instruments). After stabilization (20 min), (+)-**1** was injected as a bolus at 0.04, 0.63, 10, and 40 μg/kg. The doses were separated from one another by a 10 min interval to allow hemodynamic parameters to return to baseline values.

The same protocol was reproduced in three groups of rats. The first group ($n = 6$) received an iv bolus injection of vehicle (polyethyleneglycol 300 in sterile saline 0.9%, 40:60). The second group ($n = 6$) received an iv bolus injection of prazosin (0.16 mg/kg). The third group ($n = 6$) received an iv bolus injection of rauwolscine (0.63 mg/kg). The doses of prazosin and rauwolscine were chosen from a preliminarily set of experiments (see Supporting Information). After stabilization (20 min), (+)-**1** was injected iv as a bolus at 2.5 μg/kg in all animals.

Anesthetized Rats. The caudal vein of the animal was cannulated for anesthesia (60 mg/kg pentobarbital sodium, Sanofi, France) and for intravenous administration of compounds. The animals were intubated and ventilated at 60 respirations/min (2.5 mL/respiration, Ventilator model 683, Harvard) during anesthesia. The temperature of a heating pad (Homeothermic blanket control unit, Harvard Apparatus) was adjusted to 38 °C. Right femoral artery was catheterized to continuously measure arterial pressure via a pressor sensor. The right carotid artery was isolated, and an ultrasonic transit time flow probe (1VB, Transonic) was placed around it to record carotid blood flow. A left thoracotomy at level of fourth intercostal space was performed, and a flow probe (2.5 SB) was placed around the ascending aorta to measure cardiac output. The chest was closed with buckles. After stabilization (20 min), (+)-**1** was injected as a bolus at 0.04, 0.63, 10, and 40 μg/kg. The doses were separated from one another by a 10 min interval to allow hemodynamic parameters to return to baseline values.

Acknowledgment. We thank J. L. Maurel, who contributed to this project. We also thank Dr. C. Larrouquet and C. Berjaud for analytical support, V. Nguyen, J. Floutard, and S. Boyer for in vivo neuropharmacology technical support, L. Petitpas' assistance for bibliographic searches, and Dr. C. Andrianjara for conformation analysis.

Supporting Information Available: Experimental and analytical data for intermediates: **17**−**32**, affinity of compounds at hα_{2B} and hα_{2C} subtypes, NOE correlations, conformational analysis on compounds: **1**, **7**, **11**, and **15**, effects of reference α antagonists on the pressor response of (+)-**1**. This material is available free of charge via the Internet at http://pubs.acs.org.

References

(1) Hieble, J. P.; Bondinell, W.; Ruffolo, R. R. alpha- and beta-Adrenoceptors: From the Gene to the Clinic. Part 1. Molecular Biology and Adrenoceptor Subclassification. *J. Med. Chem.* **1995**, *38*, 3415–3444.

(2) α_2 Receptors are localized on the terminal and cell bodies of adrenergic pathways and α_2 heteroreceptors are found on non-adrenergic pathways: see Gilsbach, R.; Roser, C.; Beetz, N.; Brede, M.; Hadamek, K.; Haubold, M.; Leemhuis, J.; Philipp, M.; Schneider, J.; Urbanski, M.; Szabo, B.; Weinshenker, D.; Hein, L. Genetic dissection of alpha2-adrenoceptor functions in adrenergic versus nonadrenergic cells. *Mol. Pharmacol.* **2009**, *75*, 1160–1170.

(3) Starke, K. Presynaptic autoreceptors in the third decade: focus on alpha2-adrenoceptors. *J. Neurochem.* **2001**, *78*, 685–693.

(4) Marien, M. R.; Colpaert, F. C.; Rosenquist, A. C. Noradrenergic mechanisms in neurodegenerative diseases: a theory. *Brain Res. Rev.* **2004**, *45*, 38–78.

(5) The development of selective α_2 antagonists in depression has not been successful so far. For example, mirtazapine has a high affinity at several 5-HT receptors as well as H_1 sites: (a) Croom, K. F.; Perry, C. M.; Plosker, G. L. Mirtazapine: a review of its use in major depression and other psychiatric disorders. *Drugs* **2009**, *23*, 427–452. (b) Dekeyne, A.; Millan, M. J. Discriminative stimulus properties of the "atypical" antidepressant, mirtazapine, in rats: a pharmacological characterization. *Psychopharmacology* **2009**, *203*, 329–341.

(6) Idazoxan, (±)-2-(1,4-benzodioxan-2-yl)-2-imidazoline, [79944-58-4], Chapleo, C. B.; Myers, P. L.; Butler, R. C. M.; Doxey, J. C.; Roach, A. G.; Smith, C. F. C. alpha-Adrenoreceptor reagents. 1. Synthesis of some 1,4-benzodioxans as selective presynaptic alpha2-adrenoreceptor antagonists and potential antidepressants. *J. Med. Chem.* **1983**, *26*, 823–831.

(7) Rascol, O.; Brefel-Courbon, C.; Thalamas, C.; Descombes, S.; Fabre, N.; Montastruc, J. L.; Arnulf, I.; Vidailhet, M.; Bonnet, A. M.; Bejjani, B.; Agid, Y.; Peyro-Saint Paul, H. Idazoxan, an alpha-2 antagonist, and L-DOPA-induced dyskinesias in patients with Parkinson's disease. *Movement Disord.* **2001**, *16*, 708–713. No improvement was reported in another study in PD:. Manson, A. J.; Iakovidou, E.; Lees, A. J. Idazoxan is ineffective for levodopa-induced dyskinesias in Parkinson's disease. *Movement Disord.* **2000**, *15*, 336–337.

(8) Ghika, J.; Tennis, M.; Hoffman, E.; Schoenfeld, D.; Growdon, J. Idazoxan treatment in progressive supranuclear palsy. *Neurology* **1991**, *41*, 986–991.

(9) (a) Smith, A. P.; Wilson, S. J.; Glue, P.; Nutt, D. J. The effects and after effects of the alpha2-adrenoceptor antagonist idazoxan on mood, memory and attention in normal volunteers. *J. Psychopharmacol.* **1992**, *6*, 376–381. (b) Sahakian, B. J.; Coull, J. J.; Hodges, J. R. Selective enhancement of executive function by idazoxan in a patient with dementia of the frontal lobe type. *J. Neurol. Neurosurg. Psychiatry* **1994**, *57*, 120–121. (c) Coull, J. T. Alpha2-adrenoceptors in the treatment of dementia: an attentional mechanism? *J. Psychopharmacol.* **1996**, *10* (Suppl. 3), 43–48. (d) Coull, J. T.; Sahakian, B. J.; Hodges, J. R. The alpha-2 antagonist idazoxan remediates certain attentional and executive dysfunction in patients with dementia of frontal type. *Psychopharmacology* **1996**, *123*, 239–249.

(10) Schmidt, M. E.; Matochik, J. A.; Risinger, R. C.; Scheuten, J. L.; Zametkin, A. J.; Cohen, R. M.; Potter, W. Z. Regional brain glucose metabolism after acute alpha 2-blockade by idazoxan. *Clin. Pharmacol. Ther.* **1995**, *57*, 684–695.

(11) (a) Chase, T. N.; Foster, N. L.; Fedio, P.; Brooks, R.; Mansi, L.; Di Chiro, G. Regional cortical dysfunction in Alzheimer's disease as determined by positron emission tomography. *Ann. Neurol.* **1984**, *15* (Suppl), S170–S174. (b) Chase, T. N.; Foster, N. L.; Fedio, P.; Mansi, L.; Brooks, R.; Kessler, R.; Di Chiro, G. Cognitive and cerebral metabolic function in early and advanced Alzheimer's disease. *Monogr. Neural. Sci.* **1984**, *11*, 176–179.

(12) Karjalainen, A. J.; Virtanen, R. E.; Karjalainen, A. L.; Eloranta, M. M.; Salonen, J. S.; Sipilä, H. T.; Haapalinna, A. S. Fipamezole, (*RS*)-2-ethyl-2-(4-imidazolyl-1*H*)-5-fluoroindan, [150586-58-6]. EP 0618906, Oy Juvantia Pharma Ltd., 2004.

(13) (a) Savola, J.-M.; Hill, M.; Engstrom, M.; Merivuori, H.; Wurster, S.; McGuire, S. G.; Fox, S. H.; Crossman, A. R.; Brotchie, J. M. Fipamezole (JP-1730) is a potent alpha2 adrenergic receptor antagonist that reduces levodopa-induced dyskinesia in the MPTP-lesioned primate model of Parkinson's disease. *Movement Disord.* **2003**, *18*, 872–83. (b) Fox, S. H.; Lang, A. E.; Lang, A. E.; Brotchie, J. M. Translation of nondopaminergic treatments for levodopa-induced dyskinesia from MPTP-lesioned nonhuman primates to phase IIa clinical studies: Keys to success and roads to failure. *Movement Disord.* **2006**, *21*, 1578–1594 and references therein.

(14) In a pre-specified secondary analysis, fipamezole at the highest dose of tested (90 mg) showed that patients experienced a significant reduction in levodopa-induced dyskinesia as compared to placebo and a significant treatment-dose effect in the reduction of hours spent with diminished mobility ("off time"). *NeuroInvestment* October **2009**, 10.

(15) (a) Ruffolo, R. R.; Nichols, A. J.; Stadel, J. M.; Hieble, J. P. Pharmacologic and therapeutic applications of alpha 2-adrenoceptor subtypes. *Annu. Rev. Pharmacol. Toxicol.* **1993**, *33*, 243–279. (b) MacKinnon, A. C.; Spedding, M.; Brown, C. M. Alpha 2-adrenoceptors: more subtypes but fewer functional differences. *Trends Pharmacol. Sci.* **1994**, *15*, 119–123. (c) Bylund, D. B.; Eikenberg, D. C.; Hieble, J. P.; Langer, S. Z.; Lefkowitz, R. J.; Minneman, K. P.; Molinoff, P. B.; Ruffolo, R. R.; Trendelenburg, U. International Union of Pharmacology nomenclature of adrenoceptors. *Pharmacol. Rev.* **1994**, *46*, 121–136. (d) Balogh, B.; Szilagyi, A.; Gyires, K.; Bylund, D. B.; Matyus, P. Molecular modeling of subtypes (α2A, α2B, and α2C) of α2-adrenoceptor: A comparative study. *Neurochem. Int.* **2009**, *55*, 355–361.

(16) (a) Gyires, K.; Zadori, Z. S.; Török, T.; Matyus, P. α_2-Adrenoceptor subtypes-mediated physiological, pharmacological actions. *Neurochem. Int.* **2009**, *55*, 447–453. (b) Calzada, C. B.; De Artinano, A. A. Alpha-adrenoceptor subtypes. *Pharmacol. Res.* **2001**, *44*, 195–208. (c) MacDonald, E.; Kobilka, B. K.; Scheinin, M. Gene targeting-homing in on alpha 2-adrenoceptorsubtype function. *Trends Pharmacol. Sci.* **1997**, *18*, 211–219.

(17) (a) Atipamezole, 4-(2-ethyl-2,3-dihydro-1*H*-inden-2-yl)-1*H*-imidazole, [104054-27-5], Karjalainen, A. J.; Virtanen, R. E.; Karjalainen, A. L.; Kurkela, K. O. A. Substituted imidazole derivatives and their

preparation and use. Patent EP 183492, Farmos-Yhtyma Oy, 1986. (b) Virtanen, R.; Savola, J. M.; Saano, V. Highly selective and specific antagonism of central and peripheral alpha 2-adrenoceptors by atipamezole. *Arch. Int. Pharmacodyn. Ther.* **1989**, *297*, 190–204.

(18) Yohimbine, [65-19-0] Kovacs, P.; Hernadi, I. Alpha2 antagonist yohimbine suppresses maintained firing of rat prefrontal neurons in vivo. *NeuroReport* **2003**, *14*, 833–836.

(19) (a) Mayer, P.; Imbert, T. alpha2-Adrenoceptor antagonists. *IDrugs* **2001**, *4*, 662–676. (b) Carrieri, A; Fano, A. The in silico insights of alpha-adrenergic receptors over the last decade: methodological approaches and structural features of the 3D models. *Curr. Top. Med. Chem.* **2007**, *7*, 195–205. (c) Gentili, F.; Pigini, M.; Piergentili, A.; Giannella, M. Agonists and antagonists targeting the different alpha2-adrenoceptor subtypes. *Curr. Top. Med. Chem.* **2007**, *7*, 163–186.

(20) Some of the compounds described in this paper are included in the generic structure of the following patent: Ratilainen, J.; Huhtala, P.; Karjalainen, A.; Karjalainen, A.; Haapalinna, A.; Virtanen, R.; Lehtimaeki, J. New polycyclic indanylimidazoles with alpha2 adrenergic activity. Patent WO 2001085698, Orion Corporation, 2001. However, neither preparation nor any pharmacological data on those fused cyclopropanes are reported in this patent.

(21) (a) Ruuskanen, J. O.; Laurila, J.; Xhaard, H.; Rantanen, V.-V.; Vuoriluoto, K.; Wurster, S.; Marjamaki, A.; Vainio, M.; Johnson, M. S.; Scheinin, M. Conserved structural, pharmacological and functional properties among the three human and five zebrafish alpha 2-adrenoceptors. *Br. J. Pharmacol.* **2005**, *144*, 165–77. (b) Laurila, J. M. M.; Xhaard, H.; Ruuskanen, J. O.; Rantanen, M. J. M.; Karlsson, H. K.; Johnson, M. S.; Scheinin, M. The second extracellular loop of alpha2A-adrenoceptors contributes to the binding of yohimbine analogues. *Br. J. Pharmacol.* **2007**, *151*, 1293–1304.

(22) (a) Vacher, B.; Bonnaud, B.; Marien, M.; Pauwels, P. Novel imidazole compounds, method for preparing same and use thereof as medicines. Patent WO 2003097611, Pierre Fabre Medicament, 2003. (b) Bonnaud, B.; Funes, P.; Jubault, N.; Vacher, B. Preparation of conformationally constrained alpha2 antagonists: the bicyclo[3.1.0]-hexane approach. *Eur. J. Org. Chem.* **2005**, *15*, 3360–3369.

(23) The relative configuration at C6 was assigned on the basis of 1D NOE correlations: see Supporting Information.

(24) Berry, J. M.; Hall, L. D. Studies of specifically fluorinated carbohydrate derivatives. XVIII. Fluorinated sulfonates: ether formation using benzyl and methyl trifluoromethanesulfonate (triflate). *Carbohydr. Res.* **1976**, *47*, 307–310.

(25) (a) Parikh, J. R.; Doering, W. v. E. Sulfur trioxide in the oxidation of alcohols by dimethyl sulfoxide. *J. Am. Chem. Soc.* **1967**, *89*, 5505–5507. (b) Chen, L.; Lee, S.; Renner, M.; Tian, Q.; Nayyar, N. A simple modification to prevent side reactions in Swern-type oxidations using $Py \cdot SO_3$. *Org. Process Res. Dev.* **2006**, *10*, 163–164.

(26) van Leusen, A. M.; Schaart, F. J.; van Leusen, D. Chemistry of sulfonylmethyl isocyanides. 18. Synthesis of 1-isocyano-1-tosyl-1-alkenes and their use in the preparation of imidazoles. *J. R. Netherlands Chem. Soc.* **1979**, *98*, 258–262.

(27) Cusack, N. J.; Reese, C. B.; Risius, A. C.; Roozpeikar, B. 2,4,6-Tri-isopropylbenzenesulfonyl hydrazide: a convenient source of di-imide. *Tetrahedron* **1976**, *32*, 2157–2162.

(28) Mayr, H.; Dogan, B. Selectivities in ionic reductions of alcohols and ketones with triethylsilane/trifluoroacetic acid. *Tetrahedron Lett.* **1997**, *38*, 1013–1016.

(29) Denmark, S. E.; Edwards, J. P. A comparison of (chloromethyl)- and (iodomethyl)zinc cyclopropanation reagents. *J. Org. Chem.* **1991**, *56*, 6974–6981.

(30) The three α_1 adrenergic receptor subtypes are widely coexpressed and have similar signaling. For convenience, we used the α_{1b} subtype for in vitro tests, see: (a) Alexander, S. P. H.; Mathie, A.; Peters, J. A. Guide to receptors and channels (GRAC), 3rd ed. *Br. J. Pharmacol.* **2008**, *153*, S1−S209. (b) Chalothorn, D.; McCune, D. F.; Edelmann, S. E.; Tobita, K.; Keller, B. B.; Lasley, R. D.; Perez, D. M.; Tanoue, A.; Tsujimoto, G.; Post, G. R.; Piascik, M. T. Differential cardiovascular regulatory activities of the alpha1B- and alpha 1D-adrenoceptors subtypes. *J. Pharmacol. Exp. Ther.* **2003**, *305*, 1045–53.

(31) See Supporting Information for the relative potential energy plots on the neutral and protonated forms of compounds **1**, **7**, **11**, and **15**.

(32) Guanabenz, [(2,6-dichlorobenzylidene)amino]guanidine, [5051-62-7].

(33) Halliday, C. A.; Jones, B. J.; Skingle, M.; Walsh, D. M.; Wise, H.; Tyers, M. B. The pharmacology of fluparoxan: a selective alpha2-adrenoceptor antagonist. *Br. J. Pharmacol.* **1991**, *102*, 887–895.

(34) Atipamezole has been reported to have negligible oral bioavailability in man: (a) Huupponen, R.; Karhuvaara, S.; Anttila, M.; Vuorilehto, L.; Scheinin, H. Buccal delivery of an alpha 2-adrenergic receptor antagonist, atipamezole, in humans. *Clin. Pharmacol. Ther.* **1995**, *58*, 506–511. (b) Heinonen, P.; Sipila, H.; Neuvonen, K.; Lonnberg, H.; Cockcroft, V. B.; Wurster, S.; Virtanen, R.; Savola, M. K. T.; Salonen, J. S.; Savola, J. M. Synthesis and pharmacological properties of 4(5)-(2-ethyl-2,3-dihydro-2-silainden-2-yl)imidazole, a silicon analog of atipamezole. *Eur. J. Med. Chem.* **1996**, *31*, 725–729.

(35) The levels of NMN are dependent on and reflect the changes in the amount of NA released into the extracellular space: (a) Wood, P. L.; Kim, H.; Altar, C. A. In vivo assessment of dopamine and norepinephrine release in rat neocortex: gas chromatography−mass spectrometry measurement of 3-methoxytyramine and normetanephrine. *J. Neurochem.* **1987**, *48*, 574–579. (b) Cosi, C.; Marien, M. Decreases in mouse brain NAD+ and ATP induced by 1-methyl-4-phenyl-1, 2,3,6-tetrahydropyridine (MPTP): prevention by the poly(ADP-ribose) polymerase inhibitor, benzamide. *Brain Res.* **1998**, *809*, 58–67.

(36) Desipramine, 10,11-dihydro-5-[3-(methylamino)propyl]-5*H*-dibenz[*b*,*f*]azepine, [50-47-5], see: Mantovani, M; Dooley, D. J.; Weyerbrock, A.; Jackish, R.; Feuerstein, T. J. Differential inhibitory effects of drugs acting at the noradrenaline and 5-hydroxytryptamine transporters in rat and human neocortical synaptosomes. *Br. J. Pharmacol.* **2009**, *158*, 1848–1856. Lapiz, M. D.; Zhao, Z.; Bondi, C. O.; O'Donnell, J. M.; Morilak, D. A. Blockade of autoreceptor-mediated inhibition of norepinephrine release by atipamezole is maintained after chronic reuptake inhibition. *Int. J. Neuropsychopharmacol.* **2007**, *10*, 827–833.

(37) (a) Rodriguez, F.; Rozas, I.; Ortega, J. E.; Meana, J. J.; Callado, L. F. Guanidine and 2-Aminoimidazoline Aromatic Derivatives as alpha2-Adrenoceptor Antagonists, 1: Toward New Antidepressants with Heteroatomic Linkers. *J. Med. Chem.* **2007**, *50*, 4516–4527. (b) Rodriguez, F.; Rozas, I.; Ortega, J. E.; Erdozain, A. M.; Meana, J. J.; Callado, L. F. Guanidine and 2-aminoimidazoline aromatic derivatives as alpha2-adrenoceptor antagonists. 2. Exploring alkyl linkers for new antidepressants. *J. Med. Chem.* **2008**, *51*, 3304–3312. (c) Rodriguez, F.; Rozas, I.; Ortega, J. E.; Erdozain, A. M.; Meana, J. J.; Callado, L. F. Guanidine and 2-aminoimidazoline aromatic derivatives as alpha2-adrenoceptor ligands: searching for structure−activity relationships. *J. Med. Chem.* **2009**, *52*, 601–609.

(38) (a) Wang, M.; Ramos, B. P.; Paspalas, C. D.; Shu, Y.; Simen, A.; Duque, A.; Vijayraghavan, S.; Brennan, A.; Dudley, A.; Nou, E.; Mazer, J. A.; McCormick, D. A.; Arnsten, A. F. T. Alpha 2A-adrenoceptors strengthen working memory networks by inhibiting cAMP-HCN channel signaling in prefrontal cortex. *Cell* **2007**, *129*, 397–410. (b) Ramos, B. P.; Stark, D.; Verduzco, L.; van Dyck, C. H.; Arnsten, A. F. T. Alpha 2A-adrenoceptor stimulation improves prefrontal cortical regulation of behavior through inhibition of cAMP signaling in aging animals. *Learn. Mem.* **2006**, *13*, 770–776. (c) Dennis, T.; L'Heureux, R.; Carter, C.; Scatton, B. Presynaptic alpha-2 adrenoceptors play a major role in the effects of idazoxan on cortical noradrenaline release (as measured by in vivo dialysis) in the rat. *J. Pharmacol. Exp. Ther.* **1987**, *241*, 642–649. (d) Valentini, V.; Cacciapaglia, F.; Frau, R.; Di Chiara, G. Differential alpha2-mediated inhibition of dopamine and noradrenaline release in the parietal and occipital cortex following noradrenaline transporter blockade. *J. Neurochem.* **2006**, *98*, 113–121.

(39) (a) Finlay, J. M.; Zigmond, M. J.; Abercrombie, E. D. Increased dopamine and norepinephrine release in medial prefrontal cortex induced by acute and chronic stress: Effects of diazepam. *Neuroscience* **1995**, *64*, 619–628. (b) Ramos, B. P.; Colgan, L.; Nou, E.; Ovadia, S.; Wilson, S. R.; Arnsten, A. F. T. The beta-1 adrenergic antagonist, betaxolol, improves working memory performance in rats and monkeys. *Biol. Psychiatry* **2005**, *58*, 894–900. (c) Berridge, C. W.; Devilbiss, D. M.; Andrzejewski, M. E.; Arnsten, A. F. T.; Kelley, A. E.; Schmeichel, B.; Hamilton, C.; Spencer, R. C. Methylphenidate preferentially increases catecholamine neurotransmission within the prefrontal cortex at low doses that enhance cognitive function. *Biol. Psychiatry* **2006**, *60*, 1111–1120.

(40) One hypothesis involves a synergy between presynaptic α_{2A} receptor blockade and inhibition of the reuptake of noradrenaline: (+)-**1**: hNET inhibition in CHO cells, $pIC_{50} = 6.82 \pm 0.04$. For a precedent, see: Gobert, A.; Cussac, D.; Lejeune, F.; Newman-Tancredi, A.; Audinot, V.; Boutin, J. A.; Carr, C.; Milligan, G.; Rivet, J. M.; Brocco, M. The novel antidepressant, S35966, is a mixed serotonin and noradrenaline reuptake inhibitor and an antagonist of alpha-2-adrenoceptors. *Eur. Neuropsychopharmacol.* **2002**, *12* (Suppl. 3), S248.

(41) Freezing the conformation of the ligand diminishes its selectivity α_2 vs α_1 compared to that of atipamezole. This represents a notable departure from a central tenet in lead optimization, see: (a) Reichelt, A.; Martin, S. F. Synthesis and properties of cyclopropane-derived peptidomimetics. *Acc. Chem. Res.* **2006**, *39*, 433–442. (b) Watanabe, M.; Hirokawa, T.; Kobayashi, T.; Yoshida, A.; Ito, Y.; Yamada, S.; Orimoto, N.; Yamasaki, Y.; Arisawa, M.; Shuto, S.

Investigation of the bioactive conformation of histamine H3 receptor antagonists by the cyclopropyl strain-based conformational restriction strategy. *J. Med. Chem.* **2010**, *53*, 3585–3593and references therein.
(42) (+)-**1** has no affinity for rat β_1 and β_2-adrenoceptors ($pK_i < 4$).
(43) Scheinin, M.; Snapir, A. G protein-coupled receptors as cardiovascular drug targets. In *G Protein-Coupled Receptors in Drug Discovery*; Lundstrom, K. H., Chiu, M. L., Eds.; Taylor & Francis: Boca Raton, FL, 2006; Vol. 4, pp 37−51.
(44) (a) Gillespie, J. S.; Muir, T. C. A method of stimulating the complete sympathetic outflow from the spinal cord to blood vessels in the pithed rat. *Br. J. Pharmacol. Chemother.* **1967**, *30*, 78–87. (b) Local NA regulation via inhibitory presynaptic α_2 receptors on sympathetic nerves terminals still operate in the pithed rat, stimulation of these receptors leads to inhibition of NA release.
(45) Rauwolscine, (16-beta,17-alpha,20-alpha)-16-carboxy-17-hydroxyyohimban methyl ester, [6211-32-1], Kobinger, W.; Pichler, L. 1- and alpha2-adrenoceptor subtypes: selectivity of various agonists and relative distribution of receptors as determined in rats. *Eur. J. Pharmacol.* **1981**, *73*, 313–321.
(46) Prazosin, 1-(4-amino-6,7-dimethoxy-2-quinazolinyl)-4-(2-furoyl)-piperazine monohydrochloride, [19216-56-9], Timmermans, P. B. M. W. M.; De Jonge, A.; Thoolen, M. J. M. C.; Wilffert, B.; Batink, H.; Van Zwieten, P. A. Quantitative relationships between alpha-adrenergic activity and binding affinity of alpha-adrenoceptor agonists and antagonists. *J. Med. Chem.* **1984**, *27*, 495–503.
(47) Other hemodynamic parameters, i.e., mean cardiac output and carotid blood flow, were not significantly modified (data not shown).
(48) Wong, W. C.; Gluchowski, C. A concise synthesis of atipamezole. *Synthesis* **1995**, 139–140.
(49) Juujaervi, P.; Parhi, S.; Karjalainen, J. Process for preparing substituted imidazole derivatives and intermediates used in the process. Patent WO 2004063168, Oy Juvantia Pharma Ltd., 2004.
(50) Wurch, T.; Colpaert, F. C.; Pauwels, P. J. G-protein activation by putative antagonists at mutant Thr373Lys alpha2A adrenergic receptors. *Br. J. Pharmacol.* **1999**, *126*, 939–948.
(51) Litchfield, J. T.; Wilcoxon, F. A simplified method of evaluating dose-effect experiments. *J. Pharmacol. Exp. Ther.* **1949**, *96*, 99–113.
(52) Tallarida, R. J.; Murray, R. B. Manual of pharmacologic calculations with computer programs, 2nd Ed.; Springer Verlag: New York, 1987.